Buoyancy Effect on Fuel Containment in a Gas-Core Nuclear Rocket

HENRY A. PUTRE*
NASA Lewis Research Center, Cleveland, Ohio

Introduction

THE gas-core nuclear rocket is a proposed space propulsion system capable of high specific impulse (1500–5000 sec) and a wide range of thrust. In the latest open-cycle concept, described by Ragsdale,[1] shown in Fig. 1, the heavy uranium fuel vapor fills the central region of an approximately spherical cavity and is surrounded by lighter, faster moving hydrogen propellant. The propellant stream is heated to about 20,000° K by thermal radiation from the fissioning fuel core. The fuel density, ρ_F, is 5–15 times the propellant density, ρ_P.

One characteristic of this concept is that some unfissioned fuel is lost because the two gases are in direct contact inside the reactor cavity. Two fuel loss mechanisms that occur are turbulent mixing and a so-called buoyancy effect. Recent experiments by Bennet and Johnson[2] in a coaxial flow cavity have shown that turbulent mixing can be reduced by proper tailoring of the inlet velocity profiles. Fuel volume fractions (VF, a measure of fuel containment) as large as 34% were obtained with propellant-to-fuel mass flow ratios, m_P/m_F, above 50. In a typical engine the low fuel velocities of about 0.01 fps, coupled with a vehicle acceleration of about $g = 0.02\ g_0$ (g_0 is the Earth gravity constant), could cause a buoyancy effect which could also reduce the fuel containment in the cavity. These flow conditions could not be simulated in the experiment which had larger velocities at 1.0 g_0; however, a significant buoyancy effect was observed.

The cavity flow is analyzed here using a Navier-Stokes equation numerical solution. The purpose of this analysis is to determine a scaling parameter for the buoyancy effect so that experimental conditions at 1.0 g_0 can be related to the engine flow conditions. The flow parameters for an engine,[1] for experiments,[2] and for this analysis are given in Table 1. The Reynolds number (Re, based on total mass flow rate and cavity diameter) and mass flow ratio were fixed at 1000 and 50, respectively, for this analysis because the numerical solution would not converge for larger values. Thus their effect was not determined in the buoyancy scaling parameter. The inlet fuel-to-propellant density ratio and velocity ratio, the cavity diameter, and the acceleration were varied. The corresponding range of the buoyancy number (B, the resulting buoyancy scaling parameter which is formulated below) is also given in Table 1. Because the calculations are limited to laminar flow at a Reynolds number of 1000 (compared to turbulent flows in the engine and experiments at $Re > 10^4$), the precise values of fuel volume fraction must still be determined experimentally. This study is concerned mainly with the trends in the calculated fuel volume fractions, and results in a range of buoyancy number values to guide future experiments.

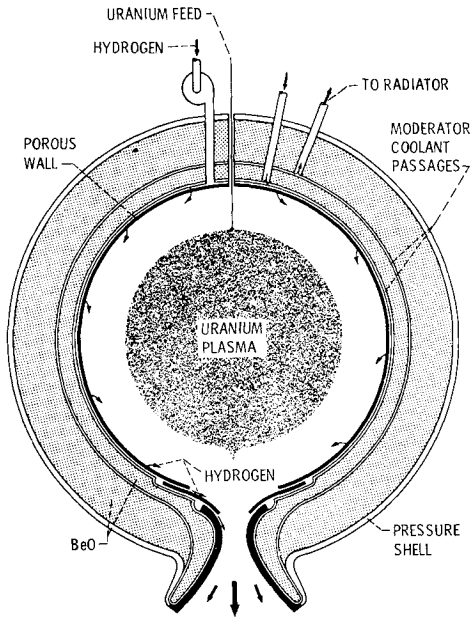

Fig. 1 Conceptual gas core nuclear rocket engine.

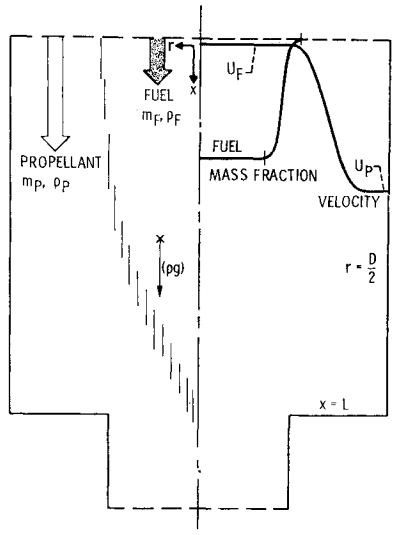

Fig. 2 Cavity model showing inlet profiles and buoyancy force.

Analysis

The cavity flow model to be analyzed is shown in Fig. 2. The analysis is for a rectangular cylinder geometry with a cavity length-to-diameter ratio, L/D, of one. This is similar to the cavity geometry of the coaxial flow experiments.[2] The assumptions of the analysis are steady, isothermal, two-fluid, viscous flow with purely axial inlet and outlet flows and with no-slip walls.

The system of equations to be solved includes the variable density Navier-Stokes equations including the acceleration body force ρg, the continuity equation, and the mass transfer equation. Details of the analysis are given in Putre.[3] An iterative solution computer code was written. This code is a modification of the basic code described by Gosman et al.,[4]

Table 1 Range of flow conditions

	Engine[1]	Coaxial flow expt.[2]	This analysis
m_P/m_F	>50	30–300	50
ρ_F/ρ_P	5–15	1.0, 4.7	1.05, 2.0, 4.0, 10
Re	10^4–10^6	2×10^5	1000
B	50–500	2–30	0–100
VF	>0.20	≤0.34	≤0.072

Presented at the 2nd Symposium on Uranium Plasmas: Research and Applications, Atlanta, Ga., November 15–17, 1971 (no paper number; published in bound volume of conference papers); submitted February 14, 1972; revision received August 2, 1972.

Index categories: Nuclear Propulsion; Viscous Nonboundary-Layer Flows.

* Nuclear Engineer, Nuclear Systems Division.

with new boundary condition, density, and velocity subroutines. Values of local mass fraction (y = local fuel density/local mixture density), also radial and axial velocities are calculated at nodes of a stretched rectangular mesh.

For inlet conditions the inlet velocity and mass fraction profiles were specified as smooth profiles with buffer layers (see Fig. 2). These are similar to the tailored profiles in the experiment of Ref. 2, and were shown in preliminary calculations to give less fuel mixing than, for example, step profiles. For outlet conditions all axial first derivatives were set to zero. The total fuel mass in the cavity is obtained by volume integration of local fuel density, $y\rho$, and the fuel volume fraction is obtained from

$$VF = \frac{\text{total fuel mass in cavity}}{\text{pure fuel density} \times \text{cavity volume}} \quad (1)$$

Results and Discussion

Numerical solutions were obtained for the analysis cases given in Table 1. The solutions would not converge for Reynolds numbers above about 1000. (Above this value the solutions become unstable even when underrelaxation was used.) In general the calculated fuel volume fractions are considerably less than the experimental values and the desired engine values. This discrepancy is partly due to the relatively low Reynolds number of the analysis. (Other exploratory calculations with this code showed, in fact, that the fuel volume fraction does increase with larger Reynolds numbers.) This discussion is thus mainly concerned with the trends in the fuel volume fractions rather than with the precise values.

The general effect of vehicle acceleration on the fuel containment is illustrated by the calculated fuel mass fraction contours in Fig. 3 for a density ratio of 2.0. Figure 3a is for zero acceleration, or $B = 0$, and Fig. 3b is for an acceleration in the range of engine values with $B = 70$. This shows that the fuel region is stretched out and becomes narrower as the acceleration increases. The net result is a decreased fuel volume fraction and a significant buoyancy effect.

Effect of density ratio at "zero-g" on fuel volume fraction

Calculations were run at fuel-to-propellant ratios of 1.05, 2, 4, and 10. The propellant-to-fuel inlet velocity ratio was adjusted over the range $U_P/U_F = 16.3$ to 183 to maintain the fixed flow ratio of 50. The fuel volume fraction decreases with increasing density ratio, as is shown in Fig. 4 for $B = 0$. This trend agrees with experiments at $1.0\,g_0$ and small B values as in Ref. 2.

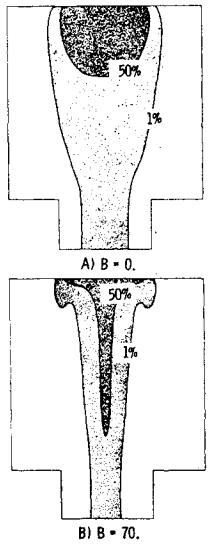

Fig. 3 Fuel mass fraction contours for different vehicle accelerations $m_p/m_F = 50$, $Re = 1000$, and $\rho_F/\rho_p = 2.0$.

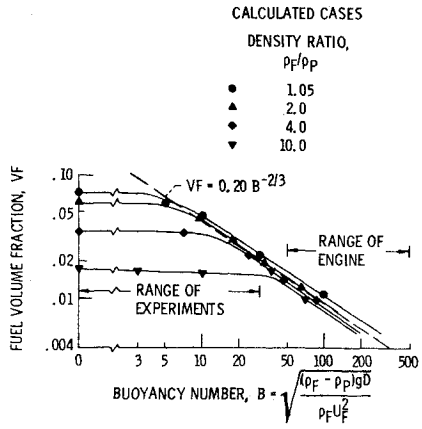

Fig. 4 Calculated fuel volume fraction as function of buoyancy number for various density ratios. $m_p/m_F = 50$, $Re = 1000$.

Effect of acceleration on fuel volume fraction

Calculated fuel volume fractions for various accelerations over the range of density ratios are plotted in Fig. 4. The vehicle acceleration was originally specified in terms of a Froude number, U_F^2/gD, which is the conventional measure of fuel inertia and acceleration forces. Values of Froude number were varied from 10^{-5} to infinity. A simplified analysis indicated that density ratio should be included in a buoyancy parameter. Several dimensionless combinations are possible. It was concluded on the basis of various crossplots and Fig. 4 that the best scaling parameter for generalizing the buoyancy effect has the form

$$B = [(\rho_F - \rho_P)gD/\rho_F U_F^2]^{1/2} \quad (2)$$

This parameter will be called the buoyancy number. The combination inside the square root is a measure of the ratio of buoyancy force to fuel inertia force. The square root is used for convenience in plotting the large range of B values.

The calculated fuel volume fractions are thus plotted in Fig. 4 as a function of buoyancy number. At a fixed density ratio the fuel volume fraction is constant for B values below about 5, and decreases as a constant power of B for large B values. Of particular importance is the fact that, for the specific combination of variables in B, the curves for various density ratios fall close together at large B values.

At buoyancy numbers above approximately 30, the fuel volume fractions for all density ratios are close to a single exponential line and may be represented by a signal correlating equation in the form

$$VF(B \geq 30) = 0.20B^{-2/3} \quad (3)$$

This line is used to extrapolate the calculations to the buoyancy number of 350 for an "0.02 g" engine with a density ratio of 10 for this engine. As shown in Fig. 4 the analysis predicts that the buoyancy effect decreases the fuel volume fraction by a factor of about 4.0. This calculated factor is subject to the limitation of the analysis. However, it indicates that a strong buoyancy effect may occur.

This reduction in fuel volume fraction should be investigated and verified in future flow simulation experiments. The buoyancy number of various engine designs will probably range from about $B = 50$ to 500, as shown in Fig. 4. By comparison, present experiments operate at buoyancy numbers less than about $B = 30$. Therefore, for accurate assessment of the buoyancy effect, the range of experimental buoyancy numbers should be extended to higher values.

Conclusions

The scaling parameter that was found to correlate the fuel volume fraction for various accelerations and various density ratios, called a buoyancy number, is given by Eq. (2). Specific

conclusions of this study are as follows: 1) at buoyancy numbers below about 5, the fuel volume fraction depends strongly on density ratio, but is independent of vehicle acceleration; 2) at buoyancy numbers larger than about 30, the fuel volume fraction is nearly independent of density ratio, and decreases with the $-\frac{2}{3}$ power of buoyancy number; 3) for a typical engine flow with a fuel-to-propellant density ratio of 10 and buoyancy number of 350, the fuel volume fraction may be reduced considerably due to buoyancy effect; 4) because of the relatively low Reynolds number of the analysis, the precise values of fuel volume fraction must be determined experimentally. Such experiments should be conducted at buoyancy numbers ranging from 50 to 500.

References

[1] Ragsdale, R. G. and Willis, E. A., Jr., "Gas-Core Rocket Reactors—A New Look," AIAA Paper 71-641, Salt Lake City, Utah, 1971.

[2] Bennett, J. C. and Johnson, B. V., "Experimental Study of One- and Two-Component Low-Turbulence Confined Coaxial Flows," CR-1851, 1971, NASA.

[3] Putre, H. A., "Effect of Buoyancy on Fuel Containment in an Open-Cycle Gas-Core Nuclear Rocket Engine," *2nd Symposium on Uranium Plasmas; Research and Applications*, AIAA, New York, 1971, pp. 189–196.

[4] Gosman, A. D., Pun, W. M., Runchal, A. K., Spalding, D. B., and Wolfstein, M., *Heat and Mass Transfer in Recirculating Flows*, Academic Press, New York, 1969.

Analytical Design of Optimal Nutation Dampers

J. C. Amieux* and M. Dureigne*
Laboratoire D'automatique et de ses Applications Spatiales du CNRS, Toulouse, France

Nomenclature

H = gyro momentum
I_i = moment of inertia about principal axis i ($i = 1, 2, 3$)
J = gyro moment of inertia about output axis
l = distance between axis 3 and ball in equilibrium position
m = mass of the ball
q = damping coefficient
r = constant defined by Eq. (1)
R = radius of curvature of tube
s = Laplace variable
α = relative angle between damper and body
Γ = spring constant
ζ = viscous damping constant
ρ = coupling factor
ω = $(I_3 - I_1)\,\omega_3/I_1$, satellite nutation frequency
ω_i = inertial angular velocity of satellite along axis i (axis 3 = spin axis)

Superscripts

( )′ = differentiation with respect to s
( )* = optimal values

Introduction

PASSIVE nutation damping of spinning satellites leads naturally to the practical problem of determining optimal parameters values. Zajac[1] and Sarychev[2] use the "maximum damping rate" criterion for the case of gravity-gradient stabilized satellites. The purpose of this Note is to show how this criterion can be applied to spinning satellites. An analytical approach is used for the practical examples of a single-degree-of-freedom gyro and a ball-in-tube damper.

Optimality Criterion

Let us assume the system under consideration has pervasive damping, so that the Hamiltonian can be used as a Liapunov function whose time derivative is $\Sigma\, Q_i\dot{q}_i$ (see Ref. 4).

For our problem this derivative is simply $-q\dot{\alpha}^2$, so that the speed of nutation decay depends only on q and $\dot{\alpha}$. For a passive damper, $\dot{\alpha}$ is maximum when the damper and satellite are tuned. In order to obtain the optimal damping coefficient q^*, we shall examine the linearized system.

Let us assume that ω_3 is constant and that the damper has only one degree of freedom. Then the linear set of equations describing the system motion is

$$\dot{\omega}_1 = -\omega\omega_2 + \rho(\alpha_{11}\omega_1 + a_{12}\omega_2 + a_{13}\dot{\alpha} + a_{14}\alpha) \tag{1a}$$

$$\dot{\omega}_2 = \omega\omega_1 + \rho(a_{21}\omega_1 + a_{22}\omega_2 + a_{23}\dot{\alpha} + a_{24}\alpha) \tag{1b}$$

$$\ddot{\alpha} = -q\dot{\alpha} - r\alpha + a_{31}\omega_1 + a_{32}\omega_2 \tag{1c}$$

where $\rho \ll 1$ is a coupling factor between the satellite and the damper and a_{ij} are constant coefficients. The characteristic equation of this system can be written as

$$f(s) = (s^2 + \omega^2)(s^2 + qs + r) + \rho(as^4 + qbs^3 + cs^2 + qds + e) \tag{2}$$

The solutions of the linear system can be written in the form

$$A_1 \exp(-\sigma_1 t)\cos(\omega_1 t + \varphi_1) + A_2 \exp(-\sigma_2 t)\cos(\omega_2 t + \varphi_2)$$

If we assume that $q \ll \omega$ and that the system is tuned, that is $r \simeq \omega^2$, the roots of $f(s)$ are very close to $+i\omega$, so that A_1 is approximately equal to A_2 and we must have $\sigma_1 = \sigma_2$ for optimal damping. If we remove the assumption of small q, it can be easily shown that statistically A_1 and A_2 have the same importance, hence we must still have $\sigma_1 = \sigma_2 = -(q/4)$. But increasing q while keeping the tuning condition will lead to an increase in the size of damper thus posing practical limitations.

Assuming that the roots of $f(s)$ are close to $\pm i\omega$ an exact root can be found using a Taylor expansion

$$f(i\omega) + f'(i\omega)ds + \tfrac{1}{2}f''(i\omega)ds^2 + 0(ds^3) = 0 \tag{3}$$

As the system is tuned (i.e., $r^* = \omega^2$), $f'(i\omega)ds$ and $f''(i\omega)ds^2$ have the same order of magnitude; thus neglecting ds^2 in Eq. (3) would lead to a large error.

A simple computation shows that Eq. (3) can be approximated by the equation with real coefficients

$$-4\omega^2 ds^2 - 2q\omega^2 ds + \rho(a\omega^4 - c\omega^2 + e) = 0$$

so that $ds = -(q/4)$ leads to

$$q^* = 2[\rho(-a\omega^4 + c\omega^2 - e)]^{1/2}/\omega \tag{4}$$

with

$$r^* = \omega^2 \tag{5}$$

It should be noted that q is a real positive number because an application of the Routh-Hurwitz criterion to $f(s)$ gives approximately $-a\omega^4 + c\omega^2 - e > 0$ as a stability condition.

It should also be noted that q can be obtained just by writing

$$f(s) \simeq (s^2 + sq^*/2 + \omega^2)^2 = 0$$

which could lead to an extension to higher order systems.

Received March 6, 1972; revision received June 12, 1972.
Index category: Spacecraft Attitude Dynamics and Control.
* Graduate Students.